

## Supporting Information

# (K,Na)NbO<sub>3</sub> Nanofiber-based Self-Powered Sensors for Accurate Detection of Dynamic Strain

*Zhao Wang,<sup>†</sup> Youdong Zhang,<sup>†</sup> Shulin Yang,<sup>†</sup> Yongming Hu,<sup>†</sup> Shengfu Wang,<sup>†</sup> Haoshuang Gu,<sup>\*,†</sup> Yu Wang,<sup>\*,‡</sup> H. L. W. Chan,<sup>‡</sup> and John Wang<sup>§</sup>*

<sup>†</sup>Hubei Collaborative Innovation Centre for Advanced Organic Chemical Materials, Faculty of Physics and Electronic Science, College of Chemistry & Chemical Engineering, Hubei University, Wuhan, Hubei Province People's Republic of China

<sup>‡</sup>Department of Applied Physics and Materials Research Centre, The Hong Kong Polytechnic University, Hong Kong SAR, People's Republic of China

<sup>§</sup>Department of Materials Science and Engineering, Faculty of Engineering, National University of Singapore, Singapore 117574, Singapore

**Corresponding Author:** guhsh@hubu.edu.cn, apywang@polyu.edu.hk

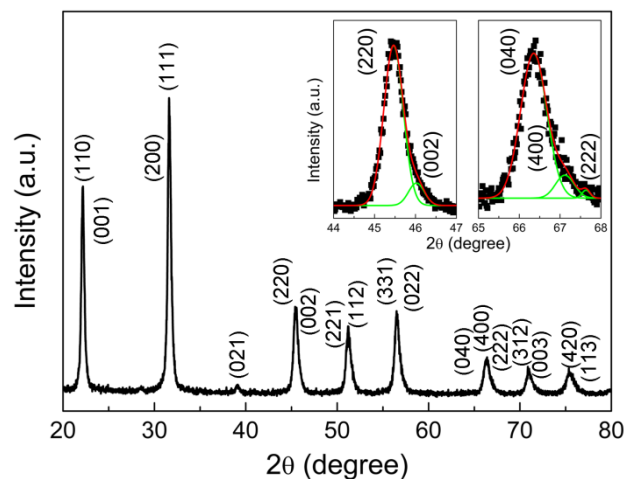


**Figure S1** XRD patterns of the KNN nanofibers synthesized by electrospinning process after annealing. The as-synthesized nanofibers are proven to be orthorhombic perovskite KNN (corresponding to JCPDS Card No. 32-0822). The lattice parameters are calculated to be  $a = 5.5762 \text{ \AA}$ ,  $b = 5.7090 \text{ \AA}$  and  $c = 3.9431 \text{ \AA}$  with the average grain size of  $25 \sim 30 \text{ nm}$ . These parameters are close to the reported value of KNN ceramics by converting them into the parameters of pseudo-monoclinic cells with  $a' = b' = 3.9902 \text{ \AA}$ ,  $c' = 3.9431 \text{ \AA}$  and  $\beta = 91.39^\circ$ , indicating no obvious size-effect in the size scale of KNN nanofibers studied in the present work.

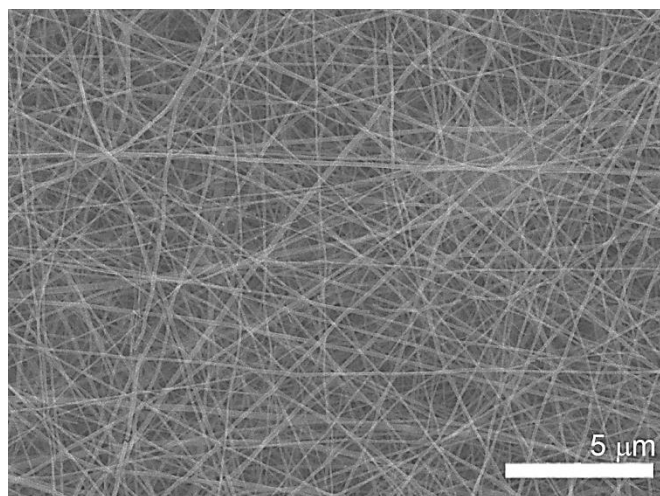


**Figure S2** SEM image of the KNN nanofibers synthesized by using the conventional flat metal as a sample collector during the electrospinning process. The as-synthesized nanofibers were randomly arranged due to the random distributed electrical field between the tip and the collector.

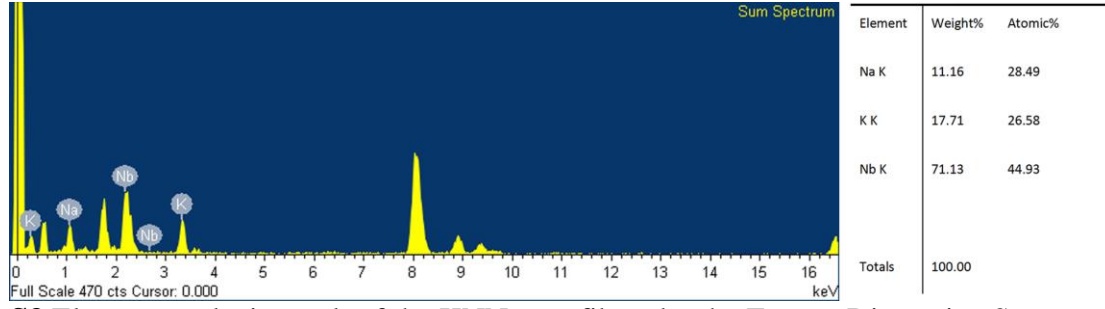


**Figure S3** Element analysis result of the KNN nanofibers by the Energy Dispersive Spectrometer. The results confirm that the composition of the sample is close to  $K_{0.48}Na_{0.52}NbO_3$ .

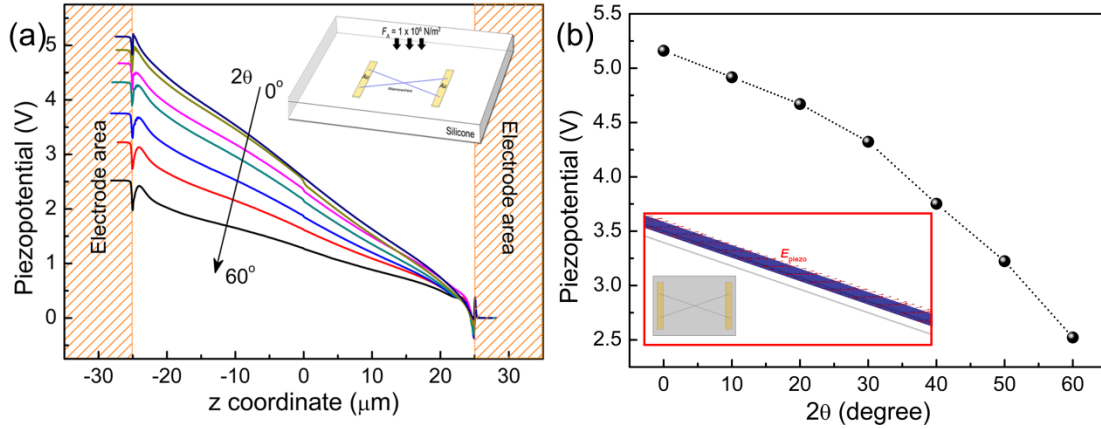


**Figure S4.** The finite element analysis results of the piezopotential generated by a pair of piezoelectric nanofibers with various interlacing angels. (a) The piezopotential distribution along the axial direction of the nanofiber. (b) The piezopotential difference between the electrodes. The model used for the FEA calculation was also shown by the inset picture. The distance between the electrodes was 50 μm. A pressure was applied on the top surface of the silicone packaging layer to induce the deformation of the piezoelectric nanomaterial. The property parameters are detailed in the experimental section. According to these results, the improvement in alignment of the nanofibers will increase the electromechanical conversion efficiency of the device. This is attributed to the decrease of poling efficiency with the decreasing poling field along the axial direction of the nanofibers as well as the decrease in deformation along the axial direction with the increasing interlacing angles.

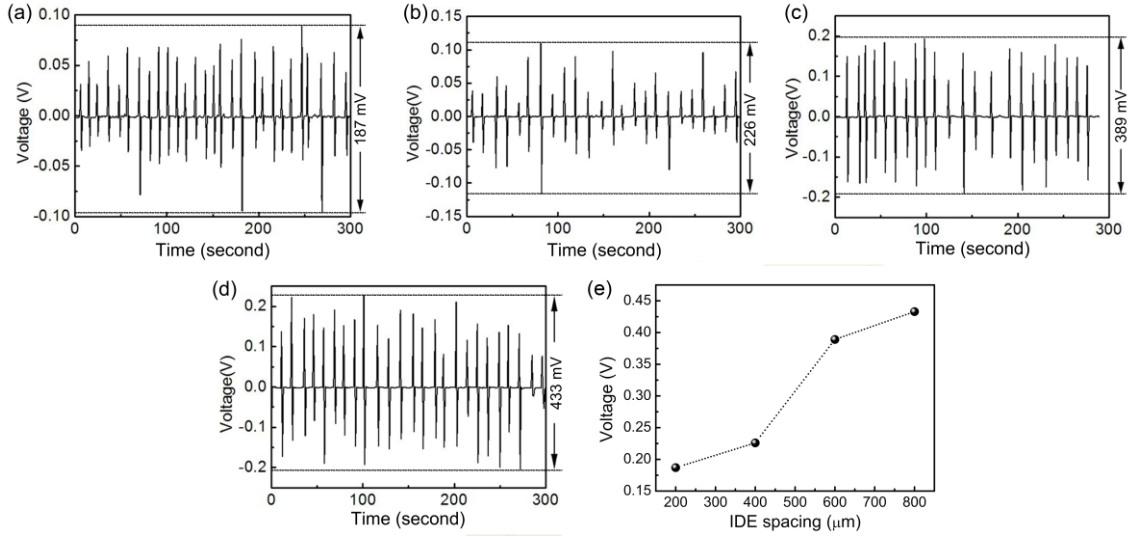


**Figure S5** The output voltage generated by the KNN strain sensor with various IDE spacing. (a) 200  $\mu\text{m}$ ; (b) 400  $\mu\text{m}$ ; (c) 600  $\mu\text{m}$ ; (d) 800  $\mu\text{m}$ ; (e) The relationship between the  $V_{pp}$  and IDE spacing. These results were obtained by applying pressures through the human fingers. As shown, the highest value of  $V_{pp}$  is increased with the IDE spacing, which is attributed to the increasing length of the nanofibers between the IDEs.

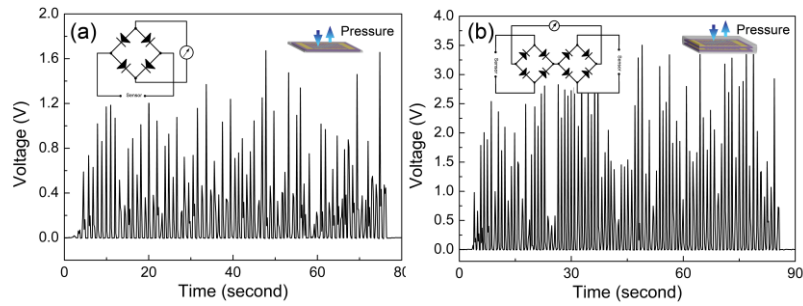


**Figure S6** The rectifying and integration of the KNN strain sensors. (a) The rectified voltage signal generated by a single sensor. (b) The voltage generated by the system consisted of two rectified strain sensor which were connected in series and integrated layer by layer. The highest output voltage of the integrated device is up to  $\sim 3.5$  V, which was approximately two times of the voltage generated by a single sensor under the pressure induced by the same person through the finger knocking.

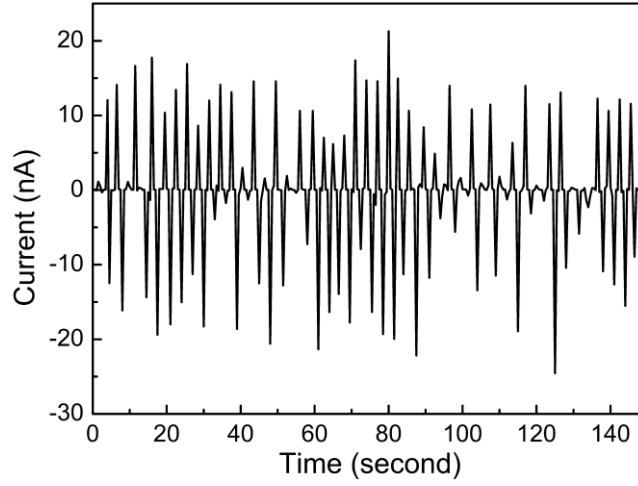


**Figure S7** The short-circuit current generated by the KNN strain sensor.

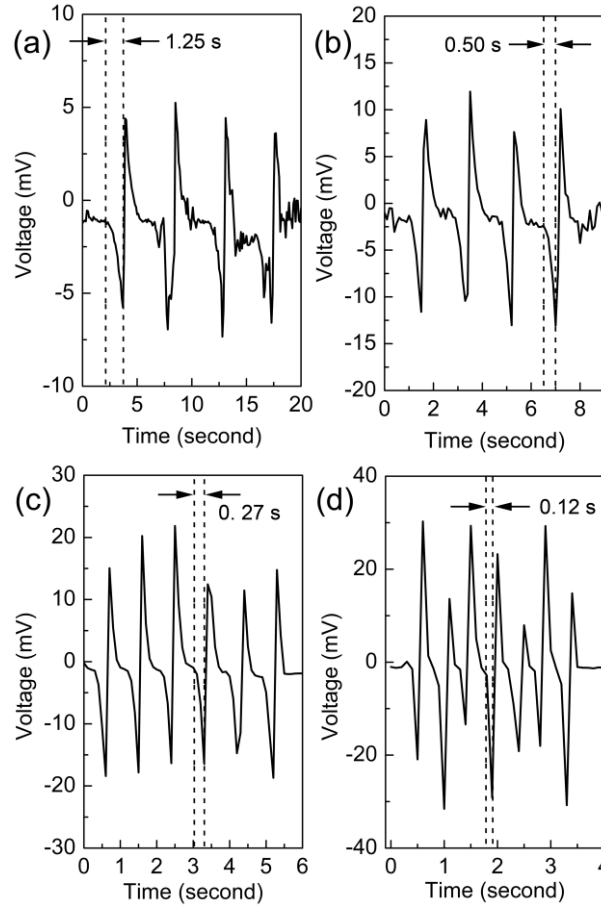


**Figure S8** The detailed voltage signal generated by the strain sensor under strain of 6 %. The time for achieve the maximum strain ( $t_{strain}$ ) can be calculated to be 1.25, 0.50, 0.27 and 0.12 s for the input vibration frequency of (a) 0.2, (b) 0.5, (c) 1 and (d) 2 Hz, respectively.

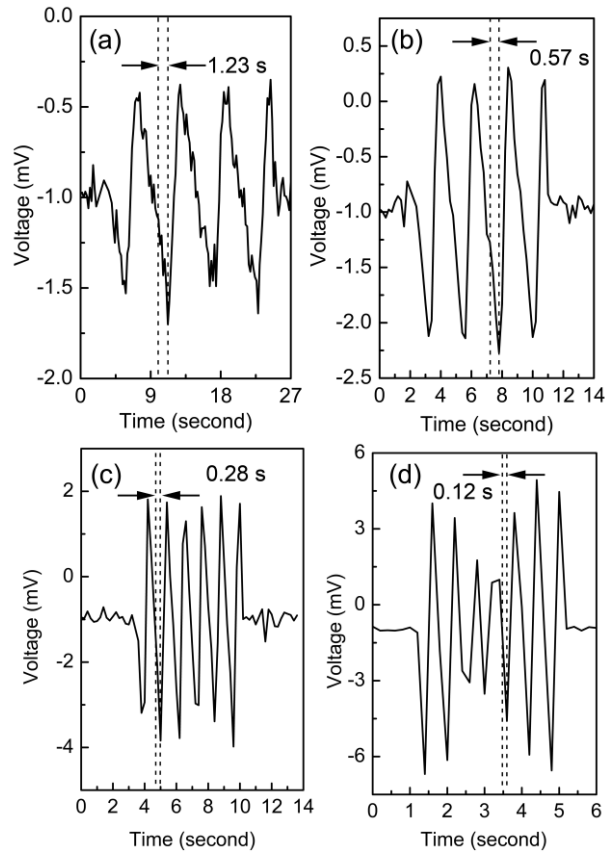


**Figure S9** The detailed voltage signal generated by the strain sensor under strain of 2 %. The time for achieve the maximum strain ( $t_{strain}$ ) can be calculated to be 1.23, 0.57, 0.28 and 0.12 s for the input vibration frequency of (a) 0.2, (b) 0.5, (c) 1 and (d) 2 Hz, respectively.

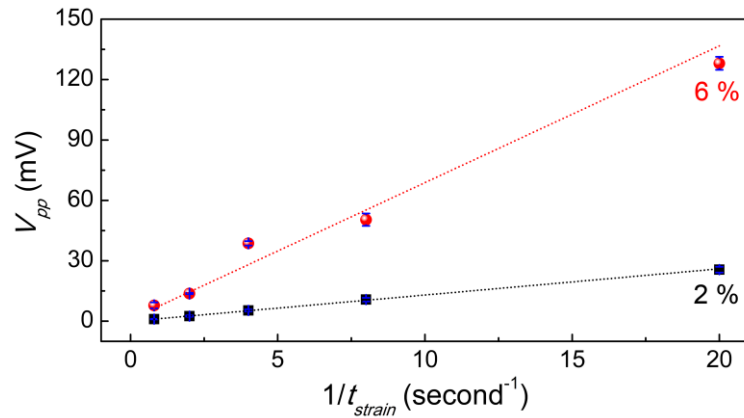


**Figure S10** The linear relationship between the peak-to-peak value of the output voltage and  $1/t_{strain}$ , which can be used for the calibration of sensing results for unperiodic strain.